International Journal of Scientific Research in Science and Technology
Print ISSN: 2395-6011 | Online ISSN: 2395-602X (www.ijsrst.com)
doi : https://doi.org/10.32628/IJSRST2310178

Backhaul Capacity-Intent Interference Easing for Sum Rate Improving in 6G Cellular Internet of Things

Murakuppam Divya*[1], Dr. G. Sreenivasulu[2]
*[1]M. Tech Student, Department of Electronics and Communication Engineering, Sri Venkateswara University College of Engineering, Tirupati, Andhra Pradesh, India
[2]Professor, Department of Electronics and Communication Engineering, Sri Venkateswara University College of Engineering, Tirupati, Andhra Pradesh, India

ARTICLEINFO

Article History:
Accepted: 05 Feb 2023
Published: 25 Feb 2023

Publication Issue
Volume 10, Issue 1
January-February-2023

Page Number
542-552

ABSTRACT

A mmWave-enabled integrated access backhaul (IAB) network for the 6G cellular Internet of Things (IoT) is necessary to handle the escalating wideband communications needs. A decreased sum rate and low successful transmission probability were the results of the mmWave-enabled IAB network's significant interference problems between access links and differentiated small-cell base stations' backhaul capacities. This article suggests the Q-learn JUP algorithm, which stands for joint user equipment association and power allocation. In order to establish the UA and PA problem, we first investigate how the SBSs-UE association and transmit power are related. Second, using the interference and backhaul burden as the state, UA and PA as the action, and the overall sum rate increment as the reward function of Q-learning, we determine the best joint optimization framework through off-line training. In order to lessen interference and backhaul load, a new backhaul capacity and cautious matching approach utility function has also been designed. Simulation results demonstrate that, in contrast to existing algorithms, the proposed algorithm may vastly enhance the network sum rate and successful transmission probability.

Keywords: Millimeter Wave (Mmwave), Interference, Backhaul, Sum Rate, Q-Learning.

I. INTRODUCTION

Due to the increase in savvy interfaces and the impending release of brand-new technologies, the Internet of Things (IOT) technology is now advancing quickly [1]. By 2030, it's anticipated that global mobile congestion will reach 5 GB per month and independent data rates are estimated to hit 100 Gbps [2]. Millimeter-wave (mmWave) communication is the best because it can provide good spectral

efficiency (SE) along with multigigabit data rate for the 6G cellular internet of things, which is necessary to meet the goals of high data rate requirements for new IOT services like virtual reality (VR), augmented reality (AR), and mixed reality (MR) [3]–[5]. Although there are certain challenges in scaling out millimetre wave-enabled ultradense networks (UDN), the two biggest ones are the severe interbeam interference and the enormous backhaul strain.

A novel integrated access and backhaul (IAB) framework was suggested in the third generation partnership project's version sixteen to address these issues [8]. The two access and backhaul links in this are built on the same network infrastructure and have millimetre wave bands as their foundation [9].

There are two significant problems in the mmwave-enabled IAB networks. One is the interference mitigation challenge, and the other is the backhaul capacity-aware problem [8]. Congestion control between backhaul links and access links depends on backhaul capacity. Backhaul capacity-aware concerns can be resolved by the backhaul capacity-aware user equipment association (UA) [10], [11]. And the power control approach is employed to lessen the interference However, the UA will be impacted by the new power allocation technique (PA) due to the ongoing relationship between the transmit power and the SBSs-UE association. To relieve backhaul strain and reduce interference, a joint UA and PA (JUP) method must be planned.

The JUP algorithm was split in to 2 problems: a UA problem, where a many-to-many matching model is used to match the number of UEs with the number of SBSs, and the PA problem, where the successive convex approximation (SCA) approach is used to allocate the power and the number of mathematical iterations keeps going until it hits the Karush-Kuhn-Tuker (KKT) point [12].

The JUP algorithm still has numerous drawbacks despite solving some issues. The sum rate obtained does not meet the high data rate requirements, the successful transmission probability obtained is only modest, the successive convex approximations (SCA) approach requires more mathematical iterations, and interference reduction as well as backhaul burden reduction should be accomplished successfully.

The Q-learning approach is a reinforcement learning algorithm without models. As a result, the problems with the JUP algorithm were solved by combining it with the Q-learning algorithm, and the new "Q-learning JUP algorithm" is now used to achieve effective sum rate, transmission probability, low computational complexity, and interference reduction with reduced backhaul burden.

The rest of the article is divided into the following sections: The system model of a millimetre Wave enabled IAB network system with such a constrained backhaul capacity is introduced in Section II. In Section III, the Q-learn joint user equipment association and power allocation algorithm is proposed to optimise the problem of interference and backhaul burden. The Q-learn JUP identifies the environment as an mmWave-enabled IAB network, the state as interference and backhaul burden, the action as UA and PA, and the goal as maximising the sum rate. In order to lessen interference and backhaul load, a new backhaul capacity and cautious matching approach utility function have also been designed for the long-term benefits. In Section IV, detailed simulation results are discussed to evaluate the performance of the proposed Q-learn joint user equipment association and power allocation algorithm. Section V stands as the article's conclusion.

II. SYSTEM MODEL

The downlink mmWave transmission framework of a two-tier heterogeneous network with a macro base station (MBS) that is densely covered by a collection of M cache-enabled SBS is the specific focus of this work. The MBS is represented by the index 0, the SBSs by the set M= {1, 2..., M} and the UEs by the set I= {1, 2..., I}. The MBS and core network are connected by a wired link. The backhaul link is the link that connects the MBS and SBSs, while the access

link is the link that connects the SBS and UEs. A backhaul link connects the SBSs to the MBs, and they provide service to a group of UEs. The UEs as = {1, 2..., I} ⊂ I, where m ϵ M, are assumed to be distributed equally and randomly within each tiny cell, according to our assumption [13]. Keep in mind that SBSs are widely dispersed and that they can overlap, thus more than one SBS may be able to provide service to a single UE.

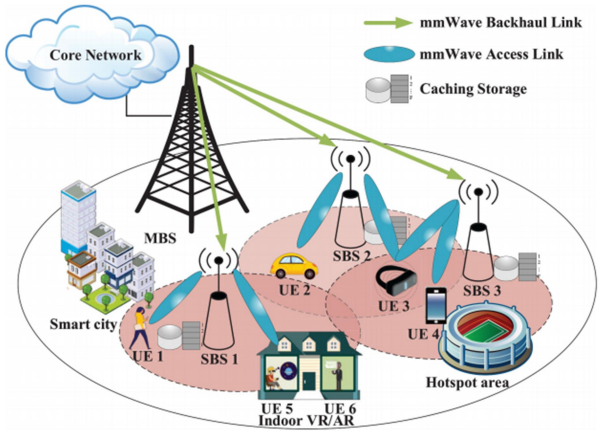

Figure 1: Typical mmWave- enabled IAB architecture

A. mmWave Communication Model

Both mmWave and sub-6 GHz bands can be effectively transmitted on using the MBS. The mm-wave band will be our main focus in this paper. The two MBSs and SBSs are capable of positioning multiple-phased antenna arrays to produce various beams that aid in space-division multiple access (SDMA) communication. This article examined the case of numerous beams transmitting simultaneously and how UEs with multi connectivity capabilities can connect with various SBSs.

1) Access Link

Effective data transfer is ensured by the use of directed beamforming technology on each link. In the suggested multibeam concurrent transmission paradigm, both intracell and intercell interferences are analysed.

Assume that the main lobe gain, side lobe gain, and main lobe beamwidth of each SBS's antenna have the same beam pattern $\emptyset(G_{ML}^t, G_{SL}^t, \theta^t)$, which includes the three variables. Consider where every SBS's antenna utilizes the identical beam pattern $\emptyset(G_{ML}^t, G_{SL}^t, \theta^t)$, which includes overall principal lobe gain G_{ML}^t, minor lobe gain G_{SL}^t, and principal lobe beamwidth θ^t. Similar to that, $\emptyset(G_{ML}^r, G_{SL}^r, \theta^r)$ designates the beam pattern of every UE. Therefore, the effective antenna gain from SBS_m to UE_i is defined as a $G_{m,i}=G_{ML}^t G_{ML}^r$ $\forall_m \in$ M and i ∈ I. Let's consider that $b_{m,i}^t$ and $b_{m,i'}^t$ stand for the two transmit beams that SBS_m uses to serve UE_i and its neighbour $UE_{i'}$. Similar to this, $b_{m,i}^r$ and $b_{m,i'}^r$ stand for the respective received beams of UE_i and $UE_{i'}$ via SBS.

Intracell interference: Intracell interference occurs whenever the primary lobes of transmit beams $b_{m,i}^t$ and $b_{m,i'}^t$ partly overlap within a cell.

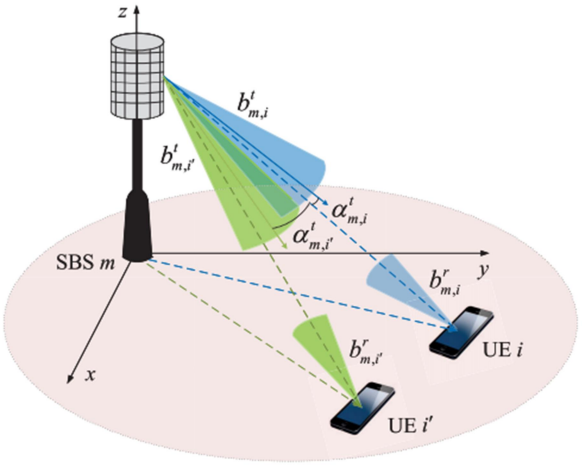

Figure 2: Intracell interference

$$G_{m,i'\to m,i}^{I_{Intra}}(\alpha_{m,i'}^t, \alpha_{m,i}^t) = \begin{cases} \frac{G_{ML}^t.\theta_{m,i,i'}^{over} + G_{SL}^t(\theta^t - \theta_{m,i,i'}^{over})}{\theta^t}.G_{ML}^r, \Delta\alpha_{m,i'\to m,i}^t \geq \theta^t \\ G_{SL}^t.G_{ML}^r.\Delta\alpha_{m,i'\to m,i}^t \leq \theta^t \end{cases} \quad (1)$$

Intercell Interference: The intracell interference occurs between the neighbouring cells, that is between SBS_m and $SBS_{m'}$. The effective antenna gain of the intercell interference link can be given by

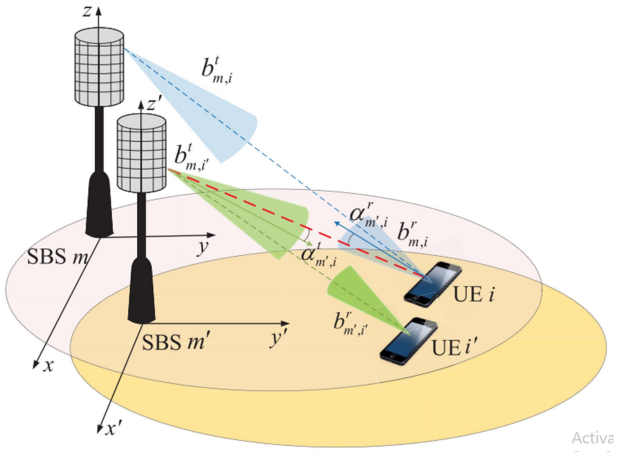

Figure 3: Intracell interference

$$G^{I_{Inter}}_{m',i'\to m,i}(\alpha^t_{m'i,}, \alpha^r_{m',i}) = \begin{cases} G^t_{ML}G^r_{ML}, \alpha^t_{m'i,} \le \frac{\theta^t}{2}, \alpha^r_{m',i} \le \frac{\theta^r}{2} \\ G^t_{ML}G^r_{SL}, \alpha^t_{m'i,} \le \frac{\theta^t}{2}, \alpha^r_{m',i} > \frac{\theta^r}{2} \\ G^t_{SL}G^r_{ML}, \alpha^t_{m'i,} > \frac{\theta^t}{2}, \alpha^r_{m',i} \le \frac{\theta^r}{2} \\ G^t_{SL}G^r_{SL}, \alpha^t_{m'i,} > \frac{\theta^t}{2}, \alpha^r_{m',i} > \frac{\theta^r}{2} \end{cases} \quad (2)$$

The intercell interference created by the nearby $SBSs_{m'}$ may cause problems for the UE_i. Line-of-sight (LOS) and nonline-of-sight (NLOS) path-loss characteristics must be taken into account since mmWave communication lines are susceptible to physical barriers from structures and even human bodies.

2) *Backhaul Link*

Assume that the MBS has a wide antenna array with A^l antennas and that the beamforming group size is A^g in order to provide the backhaul for SBSs. According to [14], $([A^l - A^g + 1]/A^g)$ can be used to calculate the beamforming gain. In a beamforming group, dedicated beams operating in the same frequency band B_b serve the SBSs. Additionally, zero-forcing beamforming is taken into account for the massive MIMO downstream transmission in order to successfully remove inter SBS interference inside a beamforming group, as had also been demonstrated in [14]. As a nutshell, $R_{0,m}$ represents the attainable data rate of a backhaul link from MBS 0 to SBS_m.

$$R_{0,m} = B_b log_2\left(1 + \frac{A^l - A^g + 1}{A^g}\frac{P_{0,m}G_{0,m}h_{0,m}L^{-1}_{0,m}}{B_b N_0}\right) \quad (3)$$

B. Caching Model

The bandwidth limitation continues to limit the network capacity of the rollout of millimetre wave backhaul. The caching technique has been carefully examined as a useful way to lessen the backhaul strain of SBSs in several contexts [15]-[17]. For the purposes of this article, we'll postulate all UEs randomly seek resources from the library F = {1, 2, . . , F}. Those resources have various dimensions, as such as S = {s_1, s_2, . . , s_F}, taking into account the variety of services. A finite memory s_m (1 < s_m<< F) cache is included with each SBS.

We take into account the hybrid caching approach utilised in [15], that potentially strike effective compromise among storing one of most popular contents (MPCs) while maintaining content diversity (DC). Each SBS's cached memory s_m is divided into two segments in particular. By taking up s_m cached memory, when 0 ≥ η ≥ 1, the MPC segment is used to cache the MPCs. The DC segment is based on a probabilistic caching model, in which the SBSs sequentially cache content f with probability q_f for all f ϵ F and occupy the surplus caching space (1-η) s_m [18].

C. Problem Formulation

By concurrently optimising the UA and the PA at SBSs in the mmWave-enabled IAB network, our aim is to improve the network's sum rate and successful transmission probability.

$$P_1: \max_{X,P} \sum_{m\in M}\sum_{i\in I} x_{m,i}R_{m,i} \quad (4a)$$

$$s.t. \sum_{i\in I} x_{m,i} \le Q_m, \sum_{m\in M} x_{m,i} \le Q_i \forall_m \in M, i \in I \quad (4b)$$

$$P_{m,i} \ge 0, \sum_{i\in I} P_{m,i} \le P^{max} \quad \forall_m \in M, i \in I \quad (4c)$$

$$\sum_{i\in I}\sum_{f\in F} x_{m,i}\, p_f(1 - c_{m,f})\, R_{m,i} \le R_{0,m}\, \forall_m \in M \quad (4d)$$

$$x_{m,i} \in \{1,0\} \quad \forall_m \in M \quad \forall_i \in I \quad (4f)$$

Every SBS_m must be able to service a maximum of Q_m UEs simultaneously, and each UE_i can only associate with a maximum of Q_i SBSs, corresponding to the spatial reuse constraint (4b). The transmit power is nonnegative according to constraint (4c), and each SBS_m maximum consuming power is P^{max}. Constraint (4d) states that its backhaul utilization of uncached resources shall not be greater than the backhaul capacities $R_{0,m}$ for each SBS. The required minimum data rate for each UE is specified by constraint (4e). The SBS-UE association choice $x_{m,i}$ is a binary variable, according to constraint (4f).

A mixed-integer nonlinear nonconvex programming problem, issue P_1 is nevertheless. Decoupling issue P_1 into two smaller-dimensional subproblems allows it to be tackled one at a time [19]–[22]. P decouples into two related but distinct subproblems as a result: Subproblems include: 1) UA and 2) PA [12]. We provide a combined user equipment association and power allocation algorithm based on Q-learning in the following section with the aim of maximising the sum rate of the network.

III. PROPOSED Q-LEARN JOINT RESOURCE ALLOCATION SCHEME

In order to address the problem P_1 and maximise the network's sum rate, a Q-learn joint resource allocation method is proposed in this section. The first task is to discuss Q-learning, which is the most well-known model-free reinforcement learning algorithm employed in this article. Through interaction with the mmWave-enabled IAB network environment, an agent learns to do actions that would provide the highest cumulative reward. We first create a Q-learning model based on state variables in the mmWave-enabled IAB network. Following that, the Q-learning model states that the algorithm's purpose is to learn an optimal strategy that takes benefit of the entire anticipated reward, which is determined by Bellman's equation. The Q-learn JUP method also provides the precise actions taken to optimise the objective function.

A. *Reinforcement Learning*

A reward mechanism is used in reinforcement learning, such as Q-learning, to represent the interaction with the environment [23]. The mechanism of learner-environment interaction is outlined in Figure 4. In such a scenario, the Q-learning model also consists of a learner, a collection of system states, S, and a set of actions, A, for each state. The learner receives a reward R for acting in a certain state, and the goal of this article is to maximise the sum rate through joint user equipment association and power allocation.

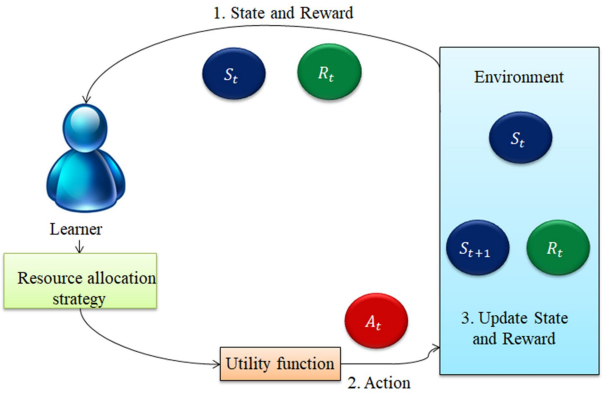

Figure 4: Q-learning based resource allocation

In our Q-learning model, which will be discussed in the next subsections, we must determine the action, state, and reward functions in order to acquire the optimal attainable policy.

System states (S): The learner relies their decision-making on the states of the mmWave downlink transmission, which are an abstraction of the mmWave-enabled IAB environment. Backhaul burden at the backhaul link and interference at the access link are the major factors that impact the state of the network environment. Furthermore, there is a connection between transmission power and the SBS-UE association. The system state S is therefore described as

$$S = S(M, I, D) = \{S_0, S_1, \ldots, S_t, \ldots, S_T\} \quad (5)$$

Where M = {1, 2, . . . , M} represents the set of SBS, I = {1,2, . . . , I} represents the set of UEs, and D = $\{D_1, D_2, \ldots, D_m\}$ represents the set of transmit power.

S_t is the system state at time t, and T is the termination time.

Action space (A): The learner takes action by observing the network's state and causes it to operate in a new state to change the network's current state. According to the context, the action refers to the power allocation (PA) to reduce interference and the user equipment association (UA) to increase backhaul capacity based on the network's state. Consequently, the expression for the set of all actions is

$$A = A(I, D) = \{A_1, A_2, \ldots, A_t, \ldots, A_T\} \quad (6)$$

Where A_t represents the action taken by the learner at time slot t, I = {1, 2, . . . , I}, and D = $\{D_1, D_2, \ldots, D_m\}$ represents the UEs association and the power allocation action at time t, respectively.

Reward function (r): The learner in this mmWave-enabled IAB system strives to maximise the accumulated rewards by performing a set of actions that directly influence the system's performance enhancement. Maximizing the system sum rate is the aim of optimization problem P_1 . The difference between the current system sum rate and the prior one is how we define the immediate reward. The immediate reward is positive as the sum rate rises. The immediate reward is negative if the sum rate falls. When a specific action is taken, the learner will be rewarded or penalised, and the mmWave-enabled IAB system's state will change. As a result, the learner is rewarded positively when their action enhances the value of the objective function. On the other hand, a penalty, or a negative reward, will lower the total rewards. A strategy track can be used to describe how the learner and the environment interact.

$$\tau = S_0, A_1, S_1, r_1, A_2, \ldots., A_t, S_t, r_t, A_{t+1}, S_{t+1}, \ldots. \quad (7)$$

B. System Utility Function

A utility function describes long-term advantages, as contrast to the reward, which just identifies what is beneficial in the here-and-now. A novel SBS-UE association pairing will affect the performance of the network of the remaining pairings since it will change the traffic load condition for SBSs and the aggregated interference among access links. To minimise the backhaul load, each SBS also gives preference to the cache hit UEs. By taking these factors into account, we propose a compensation technique for increased traffic balancing and interference in the network. The utility criteria for SBSs and UEs' backhaul capacity and interference easing are therefore defined as follows.

Utility Function of UE: The UE must be connected to the SBS with the greatest bit rate or backhaul capabilities.

Utility Function of SBS: Every SBS selects UEs which will maximize its network's sum rate while reducing overall interference with many other access links as well as the backhaul load.

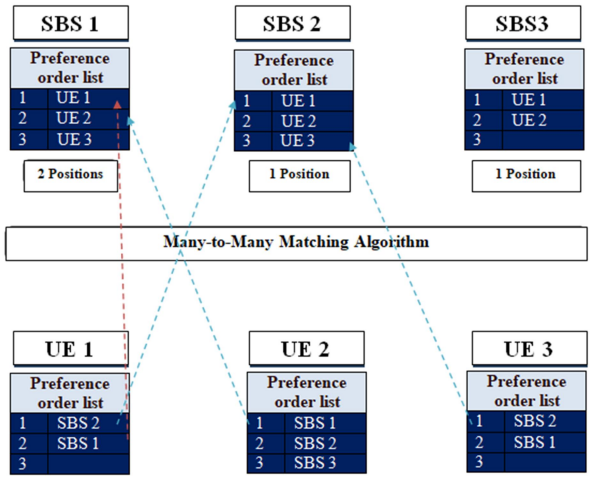

Figure 5: The UE and SBS matching based on utility functions

Although the UE and SBS utility functions mentioned above are theoretical, in reality the Q-learning algorithm must learn from the environment.

The user must learn the optimal course of action by contact with the environment because they are unaware of the average performance of the available network. The projected total return is maximised as a result of the system taking a sequence of actions $\{A_1, A_2, A_3, \ldots, A_t\}$, to solve this learning issue mathematically. As of the time t state, the accumulated rewards R are expressed as,

$$R_t(S, A, A') = \sum_{j=0}^{T} r_{t+j} \quad (8)$$

In the RL problem, the state value function $V_\pi(S,A)$ and the action-state value function $Q_\pi(S,A)$ are the two value functions used to describe the feedback from each decision.

The value of the predicted state is given as

$$V_\pi = E_\pi\{\sum_{j=0}^{T}\gamma^j R_{t+j+1}|S_t = S\} \quad (9)$$

where the mathematical expectation is signified by E {∗}. so that the maximum state value is

$$V_* = V_\pi = \max_{a\epsilon A}[R_{t+1} + \gamma V_*] \quad (10)$$

Where γ value, which ranging from 0 to 1, represents the reward discount factor, which takes into account both the value of the immediate reward and the cumulative reward. Future rewards are ignored by the learner when γ = 0, but they are deemed equally essential to current rewards when γ = 1.

After the action is performed, the expectation of the future return can be determined based on the state S at the time t, which signifies the state-action value function.

$$Q_\pi(S,A) = E_\pi[R_t|S_t = S, A_t = A] = E_\pi[R_{T+1} + \gamma Q(S',A')|S,A] \quad (11)$$

Formula for iteratively updating a state-value function

$$Q_{t+1}(S,A) = Q_t(S,A) + \alpha[R^A_{S\to S'} + \gamma max Q_t(S',A') - Q_t(S,A)] \quad (18)$$

the learning rate, A, which spans from 0 to 1,

A decision-making strategy is a set of explicit actions carried out in response to a given state, i.e., $\pi = \pi(A|S)$ for all state-action pairs. Maximizing the total reward across all states is the optimal course of action π^*. Thus, the optimal state-action value of state S is described as

$$A^* = arg\max_A Q^*(S,A) = \max_A Q(S,A) \quad (13)$$

The learner adopts a state-action to steer its decision-making in order to enhance the long-term utility of the system. The optimal course of action is to build up the greatest possible reward. The optimal approach for allocating power and UE association to the greatest state-action value function is therefore obtained.

IV. SIMULATION RESULTS

This section evaluates the Q-learn JUP algorithm's performance by contrasting it with a number of more proven methods. Subsequently, an analysis and description of the simulation's results for the total sum rate, probability of successful transmission, and number of linked links ensues.

A. Simulation Setup

The MBS has encrusted M cache-enabled SBSs in the mmWave enabled-IAB network, and every small cell has I_m uniformly as well as randomly distributed UEs (for example, M = 10 and I_m = 10). In the MBS coverage, there are between 5 and 10 SBSs, which is congruent with the values stated in [12], [24]-[26]. The suggested Q-learn JUP algorithm's performance is also contrasted with that of five baseline algorithms that use the equal PA strategy: the JUP algorithm, MMUA, random matching, min-distance, and max-SINR algorithms.

B. Results Analysis

We give some evaluation results, their related tables, and a succinct explanation in this subsection.

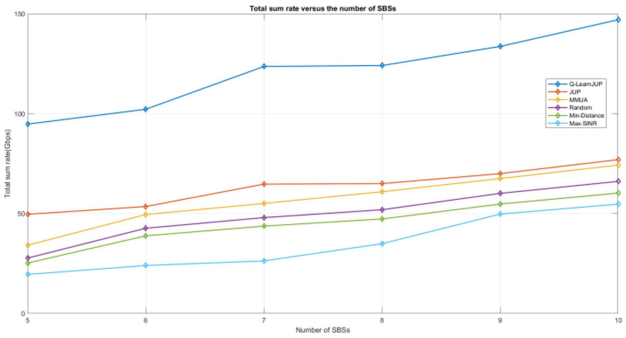

Figure 6 : Total sum rate versus the number of SBSs

The relationship between the feasible sum rate and the number of SBSs in the mmWave IAB network is depicted in Figure 6. By leveraging the backhaul resources to optimise the UA and PA, the proposed Q-learn JUP algorithm outperforms the five baseline algorithms.

TABLE I: Sum rate for different algorithms

Algorithms	Number of SBSs	Total sum rate (Gbps)
Q-learn JUP	10	147
JUP	10	77
MMUA	10	74.3
Random	10	66.1
Min-Distance	10	60.3
Max SINR	10	54.7

Compared to the remaining conventional algorithms, the proposed Q-learn JUP algorithm has a higher sum rate. When there are 10 SBSs, Table I displays the various algorithms along with the sum rates (in Gbps) that correspond to them.

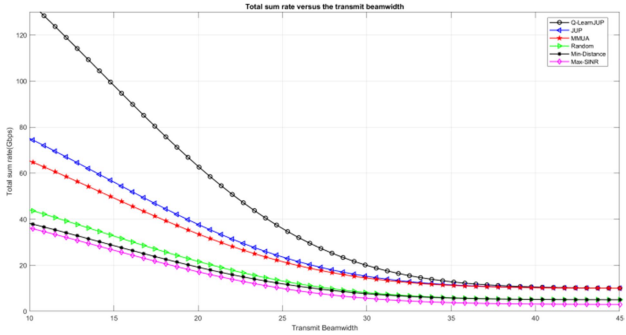

Figure 7: Total sum rate versus the transmit beamwidth

The effects of the transmitter's beamwidth on the possible sum rate are portrayed in Figure 7. Beamwidth and sum rate have an inverse relationship with one another.

TABLE II: Sum rate if beamwidth is 45 degrees

Algorithms	Transmit beamwidth (Degrees)	Total sum rate (Gbps)
Q-learn JUP	45	10.2
JUP	45	10.01
MMUA	45	10.01
Random	45	5.007
Min-Distance	45	5.006
Max SINR	45	3.006

Table II demonstrates how the sum rate of various algorithms differs at a 45-degree angle. When compared to the other standard techniques, the proposed algorithm has a maximum sum rate at a beam angle of 45 degrees.

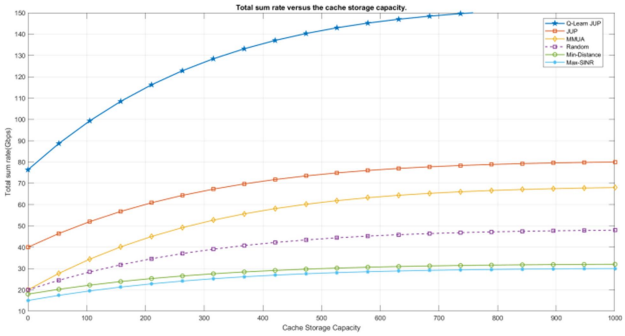

Figure 8 : Total sum rate versus the cache storage capacity

Figure 8 demonstrates that as cache store capacity grows, the network sum rate also rises. The relationship between the sum rate and cache storage is proportional. As compared to the other algorithms, the Q-learn algorithm is superior.

TABLE III: Total sum rate at cache storage

Algorithms	Cache storage capacity (Files)	Total sum rate (Gbps)
Q-learn JUP	1000	152.8
JUP	1000	80
MMUA	1000	68
Random	1000	48
Min-Distance	1000	32
Max SINR	1000	30

There is a cache in each and every SBS, and each cache has a maximum storage capacity of 1000 files [26]. The sum rate increment for various algorithms for a fixed cache store capacity is shown in Table III.

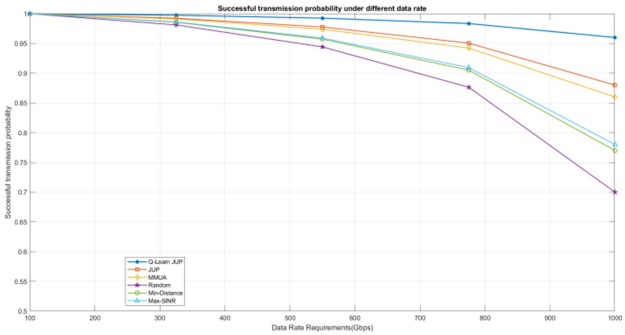

Figure 9: Successful transmission probability under different data rate requirements

The probability of a successful transmission is displayed in Figure 9 for various algorithms. The proposed algorithm is more successful than the other algorithms.

TABLE IV: Successful transmission probability for different algorithms

Algorithms	Data rate requirements (Mbps)	Successful transmission probability (Percentage)
Q-learn JUP	100	96
JUP	100	88
MMUA	100	86
Random	100	70
Min-Distance	100	77
Max SINR	100	78

Table IV shows the successful transmission probability for a data rate of 100 Mbps.

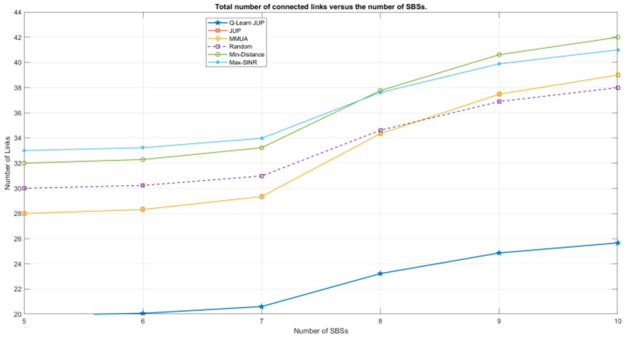

Figure 10: Total number of connected links versus the number of SBSs

According to these five methods, as the number of SBS increases in Figure 10, so do the connected links. The proposed Q-learn JUP algorithm uses both access and backhaul resources more effectively than the five baseline algorithms, which results in fewer connected links than those of the five baseline algorithms. The proposed Q-learn JUP algorithm's benefit in traffic load-balancing is becoming increasingly obvious as the number of connected links and network sum rate both keep growing.

TABLE V: The number of connected access links at varying SBSs

Algorithms	Number of SBSs		Number of links	
	At 10	At 5	At 10	At 5
Q-learn JUP	10	5	25.66	20
JUP	10	5	39	28
MMUA	10	5	39	28
Random	10	5	38	30
Min-Distance	10	5	42	32
Max SINR	10	5	41	33

The total number of connected links for 10 SBSs and 5 SBSs can be seen in Table V.

V. CONCLUSION

In order to facilitate the mmWave-enabled IAB architecture for the 6G cellular IoT, this article has proposed a Q-learn joint user equipment association and power allocation interference mitigation model with high backhaul capacity. The Q-learning algorithm is used in tandem with the joint user equipment association and power allocation method by properly indicating the environment as a mmWave-enabled IAB network, the state as interference and backhaul burden, the action as UA and PA, and the goal is to maximise the sum rate so that the reward will be positive if the sum rate increases and the probability of successful transmission increases. Simulation results demonstrated that, when compared to traditional algorithms, our proposed algorithm may vastly enhance the network sum rate and the successful transmission probability.

Many approaches of extending current work are possible. Initially, take into account the in-band frequency allocation's cross-tier interference. Finally, altering the caching model.

VI. REFERENCES

[1]. H. Song, J. Bai, Y. Yi, J. Wu and L. Liu, "Artificial Intelligence Enabled Internet of Things: Network Architecture and Spectrum Access," in IEEE Computational Intelligence Magazine, vol. 15, no. 1, pp. 44-51, Feb. 2020, doi: 10.1109/MCI.2019.2954643.

[2]. IMT Traffic Estimates for the Years 2020 to 2030, document ITU-R SG05, ITU, Geneva, Switzerland, Jul. 2015.

[3]. M. Giordani, M. Polese, M. Mezzavilla, S. Rangan and M. Zorzi, "Toward 6G Networks: Use Cases and Technologies," in IEEE Communications Magazine, vol. 58, no. 3, pp. 55-61, March 2020, doi: 10.1109/MCOM.001.1900411.

[4]. K. B. Letaief, W. Chen, Y. Shi, J. Zhang and Y. -J. A. Zhang, "The Roadmap to 6G: AI Empowered Wireless Networks," in IEEE Communications Magazine, vol. 57, no. 8, pp. 84-90, August 2019, doi: 10.1109/MCOM.2019.1900271.

[5]. B. Zong, C. Fan, X. Wang, X. Duan, B. Wang and J. Wang, "6G Technologies: Key Drivers, Core Requirements, System Architectures, and Enabling Technologies," in IEEE Vehicular Technology Magazine, vol. 14, no. 3, pp. 18-27, Sept. 2019, doi: 10.1109/MVT.2019.2921398.

[6]. C. Fiandrino, H. Assasa, P. Casari and J. Widmer, "Scaling Millimeter-Wave Networks to Dense Deployments and Dynamic Environments," in Proceedings of the IEEE, vol. 107, no. 4, pp. 732-745, April 2019, doi: 10.1109/JPROC.2019.2897155.

[7]. S. A. Busari, S. Mumtaz, S. Al-Rubaye and J. Rodriguez, "5G Millimeter-Wave Mobile Broadband: Performance and Challenges," in IEEE Communications Magazine, vol. 56, no. 6, pp. 137-143, June 2018, doi: 10.1109/MCOM.2018.1700878.

[8]. "NR; study on integrated access and backhaul, V16.0.0," 3GPP, Sophia Antipolis, France, Rep. TR 38.874, Jan. 2018.

[9]. W. Pu, X. Li, J. Yuan and X. Yang, "Resource Allocation for Millimeter Wave Self-Backhaul Network Using Markov Approximation," in IEEE Access, vol. 7, pp. 61283-61295, 2019, doi: 10.1109/ACCESS.2019.2915968.

[10]. Q. Han, B. Yang, G. Miao, C. Chen, X. Wang, and X. Guan, "Backhaul aware user association and resource allocation for energy-constrained HetNets," IEEE Trans. Veh. Technol., vol. 66, no. 1, pp. 580–593, Jan. 2017.

[11]. F. Pervez, M. Jaber, J. Qadir, S. Younis, and M. A. Imran, "Memory based user-centric backhaul-aware user cell association scheme," IEEE Access, vol. 6, pp. 39595–39605, 2018.

[12]. Q. Zhang, W. Ma, Z. Feng and Z. Han, "Backhaul-Capacity-Aware Interference Mitigation Framework in 6G Cellular Internet of Things," in IEEE Internet of Things Journal, vol. 8, no. 12, pp. 10071-10084, 15 June15, 2021, doi: 10.1109/JIOT.2021.3050013.

[13]. M. Shi, K. Yang, Z. Han and D. Niyato, "Coverage Analysis of Integrated Sub-6GHz-mmWave Cellular Networks With Hotspots," in IEEE Transactions on Communications, vol. 67, no. 11, pp. 8151-8164, Nov. 2019, doi: 10.1109/TCOMM.2019.2939802.

[14]. N. Wang, E. Hossain and V. K. Bhargava, "Joint Downlink Cell Association and Bandwidth Allocation for Wireless Backhauling in Two-Tier HetNets With Large-Scale Antenna Arrays," in IEEE Transactions on Wireless Communications, vol. 15, no. 5, pp. 3251-3268, May 2016, doi: 10.1109/TWC.2016.2519401.

[15]. Y. Zhu, G. Zheng, L. Wang, K. -K. Wong and L. Zhao, "Content Placement in Cache-Enabled Sub-6 GHz and Millimeter-Wave Multi-Antenna Dense Small Cell Networks," in IEEE Transactions on Wireless Communications, vol. 17, no. 5, pp. 2843-2856, May 2018, doi: 10.1109/TWC.2018.2794368.

[16]. J. Gao, L. Zhao and X. Shen, "The Study of Dynamic Caching via State Transition Field—the

Case of Time-Invariant Popularity," in IEEE Transactions on Wireless Communications, vol. 18, no. 12, pp. 5924-5937, Dec. 2019, doi: 10.1109/TWC.2019.2940676.

[17].S. Zhang, P. He, K. Suto, P. Yang, L. Zhao and X. Shen, "Cooperative Edge Caching in User-Centric Clustered Mobile Networks," in IEEE Transactions on Mobile Computing, vol. 17, no. 8, pp. 1791-1805, 1 Aug. 2018, doi: 10.1109/TMC.2017.2780834.

[18].S. Zhang and J. Liu, "Optimal Probabilistic Caching in Heterogeneous IoT Networks," in IEEE Internet of Things Journal, vol. 7, no. 4, pp. 3404-3414, April 2020, doi: 10.1109/JIOT.2020.2969466.

[19].D. P. Bertsekas, Nonlinear Programming, 2nd ed. Belmont, MA, USA: Athena Sci., 1999.

[20].H. Zhang, H. Liu, J. Cheng and V. C. M. Leung, "Downlink Energy Efficiency of Power Allocation and Wireless Backhaul Bandwidth Allocation in Heterogeneous Small Cell Networks," in IEEE Transactions on Communications, vol. 66, no. 4, pp. 1705-1716, April 2018, doi: 10.1109/TCOMM.2017.2763623.

[21].H. H. M. Tam, H. D. Tuan, D. T. Ngo, T. Q. Duong and H. V. Poor, "Joint Load Balancing and Interference Management for Small-Cell Heterogeneous Networks With Limited Backhaul Capacity," in IEEE Transactions on Wireless Communications, vol. 16, no. 2, pp. 872-884, Feb. 2017, doi: 10.1109/TWC.2016.2633262.

[22].T. M. Nguyen, W. Ajib and C. Assi, "Designing Wireless Backhaul Heterogeneous Networks With Small Cell Buffering," in IEEE Transactions on Communications, vol. 66, no. 10, pp. 4596-4610, Oct. 2018, doi: 10.1109/TCOMM.2018.2837113.

[23].G. Zhao, Y. Li, C. Xu, Z. Han, Y. Xing and S. Yu, "Joint Power Control and Channel Allocation for Interference Mitigation Based on Reinforcement Learning," in IEEE Access, vol. 7, pp. 177254-177265, 2019, doi: 10.1109/ACCESS.2019.2937438.

[24].Y. -J. Yu, T. -Y. Hsieh and A. -C. Pang, "Millimeter-Wave Backhaul Traffic Minimization for CoMP Over 5G Cellular Networks," in IEEE Transactions on Vehicular Technology, vol. 68, no. 4, pp. 4003-4015, April 2019, doi: 10.1109/TVT.2019.2900379.

[25].“Study on scenarios and requirements for next generation access technology, V16.0.0,” 3GPP, Sophia Antipolis, France, Rep. TR 38.913, Jul. 2020.

[26].L. Wang, K. Wong, S. Jin, G. Zheng, and R. W. Heath, “A new look at physical layer security, caching, and wireless energy harvesting for heterogeneous ultra-dense networks,” IEEE Commun. Mag., vol. 56, no.6,pp.49–55,Jun.2018

Cite this article as :

Murakuppam Divya, Dr. G. Sreenivasulu, "Backhaul Capacity-Intent Interference Easing for Sum Rate Improving in 6G Cellular Internet of Things ", International Journal of Scientific Research in Science and Technology (IJSRST), Online ISSN : 2395-602X, Print ISSN : 2395-6011, Volume 10 Issue 1, pp. 542-552, January-February 2023. Available at doi : https://doi.org/10.32628/IJSRST2310178
Journal URL : https://ijsrst.com/IJSRST2310178